MitoNEET-dependent formation of intermitochondrial junctions

Alexandre Vernay[a], Anna Marchetti[a], Ayman Sabra[a], Tania N. Jauslin[a], Manon Rosselin[a], Philipp E. Scherer[b], Nicolas Demaurex[a], Lelio Orci[a,1], and Pierre Cosson[a,1]

[a]Faculty of Medicine, Department of Cell Physiology and Metabolism, University of Geneva, Centre Médical Universitaire, CH1211 Geneva 4, Switzerland; and [b]Touchstone Diabetes Center, Department of Internal Medicine, University of Texas Southwestern Medical Center, Dallas, TX 75390–8549

MitoNEET (mNEET) is a dimeric mitochondrial outer membrane protein implicated in many facets of human pathophysiology, notably diabetes and cancer, but its molecular function remains poorly characterized. In this study, we generated and analyzed mNEET KO cells and found that in these cells the mitochondrial network was disturbed. Analysis of 3D-EM reconstructions and of thin sections revealed that genetic inactivation of mNEET did not affect the size of mitochondria but that the frequency of intermitochondrial junctions was reduced. Loss of mNEET decreased cellular respiration, because of a reduction in the total cellular mitochondrial volume, suggesting that intermitochondrial contacts stabilize individual mitochondria. Reexpression of mNEET in mNEET KO cells restored the WT morphology of the mitochondrial network, and reexpression of a mutant mNEET resistant to oxidative stress increased in addition the resistance of the mitochondrial network to H_2O_2-induced fragmentation. Finally, overexpression of mNEET increased strongly intermitochondrial contacts and resulted in the clustering of mitochondria. Our results suggest that mNEET plays a specific role in the formation of intermitochondrial junctions and thus participates in the adaptation of cells to physiological changes and to the control of mitochondrial homeostasis.

mitoNEET | CISD1 | mitochondria | intermitochondrial junctions | endoplasmic reticulum

Mitochondria play a key role in many facets of cellular physiology, notably metabolism and the production of ATP, and storage of calcium. Mitochondrial dysfunction has been linked to a wide variety of human pathologies, including diabetes (1), neurodegeneration, and cancer (2). In many pathological situations, alterations of mitochondrial morphology resulting from changes in mitochondrial fusion and fission dynamics have been observed, and may play an important role in the development of the observed physiological anomalies (3). The molecular mechanisms ensuring the control of mitochondrial morphology are therefore under intense scrutiny, because they may represent targets for therapeutic interventions in these various pathologies. Several key elements of the fusion/fission machinery have been identified and characterized, in particular four dynamin-related proteins: mitofusin 1 and mitofusin 2, which promote fusion of mitochondrial outer membranes; optic atrophy 1, which promotes fusion of inner membranes; and DRP1, which ensures fission of outer mitochondrial membranes (4).

MitoNEET (mNEET) was originally identified as a mitochondrial binding site of pioglitazone, an insulin sensitizer (5). Although it was later revealed that the main mitochondrial binding site of pioglitazone was the Mpc mitochondrial pyruvate carrier complex (6), this initial observation launched a series of studies to unravel the molecular function of the mNEET protein. mNEET belongs to a family of three proteins exhibiting a CDGSH domain, together with miner1 and miner2. mNEET and miner2 are integral proteins of the outer mitochondrial membrane, with their CDGSH domain located in the cytosol. Miner1 is an integral protein of the endoplasmic reticulum (7). Genetic inactivation of mNEET reduces by ~30% the maximal capacity of heart mitochondria to transport electrons and carry out oxidative phosphorylation. In these experiments, no alterations in the number or morphology of mitochondria were reported (7). The CDGSH of mNEET binds a 2Fe-2S cluster that can undergo oxidation and reduction. Because of the unusual structure of the mNEET CDGSH, the FeS cluster can be released at low pH (8), and in its oxidized state, it can be transferred to an acceptor protein (9), although the functional significance of these observations remains to be determined. In addition to its putative role in diabetes, mNEET has been implicated in tumor development: mNEET and miner1 are overexpressed in breast cancer cells, and their downregulation reduces cell proliferation and tumor growth (10). mNEET has also been overexpressed experimentally in adipocytes and in pancreatic cells to modulate their physiology (11, 12). However, the exact function of mNEET remains elusive, as well as the effect of its overexpression on cellular physiology.

Overexpression of mNEET in pancreatic β cells induced the formation of mitochondrial clusters (12), raising the intriguing possibility that mNEET may participate in the control of the mitochondrial network morphology. The present study was designed to test this hypothesis. Our results suggest that mNEET is involved in the formation of intermitochondrial junctions (IMJs), thus playing an important part in the establishment of the mitochondrial network in the cell.

Significance

Mitochondria form dynamic networks in eukaryotic cells by constantly fusing with and separating from each other. Alterations in the mitochondrial network are observed in many pathological situations, such as diabetes, neurodegeneration, and cancer. In this study, we observe at the ultrastructural level the formation of direct contacts between mitochondria, called intermitochondrial junctions, by a mechanism distinct from that allowing fusion and fission of mitochondria. MitoNEET, a protein exposed at the cytosolic surface of mitochondria, controls the formation of intermitochondrial junctions. Its overexpression increases intermitochondrial junctions, whereas its absence reduces their frequency. Together, these observations reveal the existence of a new mechanism controlling the morphology of the cellular mitochondrial network and its adaptation to various physiological or pathological situations.

Results

Loss of mNEET Decreases IMJs. To test a putative role of mNEET in the establishment and maintenance of the mitochondrial network, we used the CRISPR-Cas9 method to generate mouse embryonic fibroblast (MEF) cells in which the gene coding for mNEET was genetically inactivated. The genotype of the mutant cells was determined by sequencing of the genomic DNA, and immunofluorescence staining using an anti-mNEET recombinant antibody (MRB251) confirmed the loss of the mNEET protein (7) (Fig. S1 *A* and *B*). These new tools also allowed us to confirm previous reports that endogenous mNEET is present in mitochondria (Fig. S1*C*). The general organization of the endoplasmic reticulum (ER), of the Golgi complex, and of the tubulin cytoskeleton was indistinguishable between WT and mNEET KO cells (Fig. S1*D*).

We then analyzed by fluorescence microscopy the morphology of mitochondria in parental (WT) MEFs and in mNEET KO cells expressing a mitochondrially targeted fluorescent fusion protein. Compared with parental cells, the mitochondrial network appeared less connected in mNEET KO cells (Fig. 1*A*). Because the morphology of mitochondria exhibited a significant variability from cell to cell, this observation was quantified by counting the percentage of cells with various types of mitochondrial network, from fully fragmented (type 4) to fully connected (type 2) or hyperconnected (type 1) (Fig. S2*A*). Importantly, all quantifications were done on blinded samples to reduce experimental biases. Compared with parental cells, three independent clones of mNEET KO cells exhibited a significantly less-connected mitochondrial network (Fig. 1*B*). For simplicity, in this study the degree of connectivity of the mitochondrial network was defined by a single number between 0 (no connectivity) and 200 (hyperconnected) (Fig. 1*C*), as defined in *Materials and Methods*. In live unfixed cells, a similar fragmentation of the mitochondrial network was observed in mNEET KO cells (Fig. S2*B*).
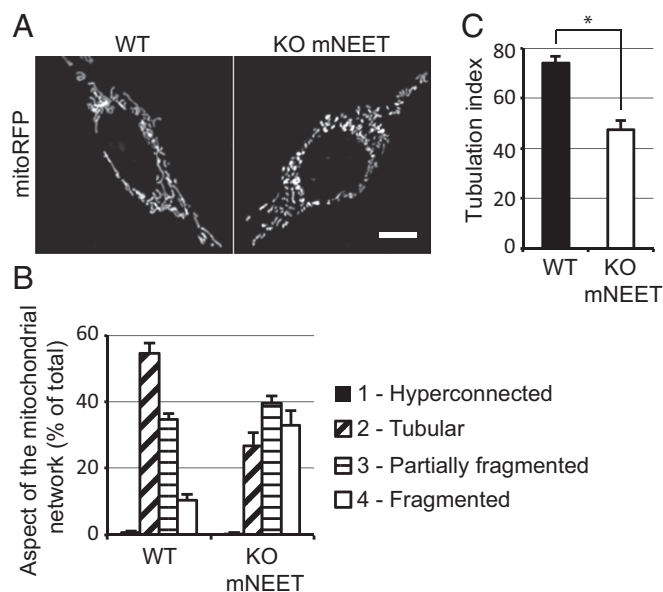
Fig. 1. Genetic inactivation of mNEET decreases connectivity of the mitochondrial network. (*A*) Mito-RFP was expressed in WT (*Left*) or in *mNEET KO* MEFs cells (*Right*) and cells were observed by fluorescence microscopy. (Scale bar, 10 μm.) (*B*) For each cell, the connectivity of the mitochondrial network was graded 4 (totally fragmented), 3 (partially fragmented), 2 (tubular), or 1 (hyperconnected). The quantification was performed on blinded samples. The average and SEM of 14 independent experiments are indicated. (*C*) The tubulation index was calculated as described in *Materials and Methods*. *$P < 0.001$ (Student *t* test).

A decrease in the connectivity of the mitochondrial network visualized by fluorescence microscopy could in principle reflect a fragmentation of mitochondria, characterized by a decrease in the size of individual mitochondria. However, the optimal resolution of classic fluorescence microscopy is 200 nm, and does not allow us to delimitate unambiguously single mitochondria. To obtain 3D reconstructions of cells with sufficient resolution, we used a dual-beam focused ion beam/scanning electron microscope (FIB/SEM). The FIB allows us to gradually trim the sample (section thickness 10 nm), whereas the scanning electron beam visualizes the milled surface with a lateral resolution of ~4 nm (Fig. 2). The pictures obtained have a lower resolution than classic transmission electron microscopy (TEM), but they allow visualization of the whole cell volume. To compare the size of mitochondria in WT and mNEET KO cells, the number of sections traversed by each individual mitochondrion was determined (z-size). Contrary to our expectations, the z-size of mitochondria in mNEET KO cells (1.33 ± 0.08 μm, $n = 103$) and in WT cells (1.25 ± 0.09 μm, $n = 106$) was not significantly different ($P = 0.48$; Student *t* test) (Fig. 2*A* and Table S1). These observations suggest that changes in the size of individual mitochondria do not account for the modification of the mitochondrial network observed by fluorescence microscopy in mNEET KO cells.

As previously reported (13), mitochondria can engage in close contacts, referred to as IMJs, and this could in principle increase the apparent connectivity of the mitochondrial network. IMJs were readily observed by FIB/SEM (Fig. 2*B*, arrowheads) and this technique also allowed us to ascertain that no fusion between mitochondria was taking place next to the regions of close contacts. To evaluate the significance of IMJs in connecting the mitochondrial network, we first determined the frequency of IMJs in WT cells. In WT cells, 52% of mitochondria were in contact with at least one other mitochondrion, and 16% with at least two. Quantification indicated that IMJs represented 0.8% of the total surface of mitochondria (Table S1). These contacts, which cannot at the fluorescence microscopy level be distinguished from fused mitochondria, would thus contribute significantly to the apparent connectivity of the mitochondrial network.

We then analyzed whether contacts between mitochondria were altered by genetic ablation of mNEET. In mNEET KO cells, contacts were significantly less abundant than in WT cells: only 34% of mitochondria participated in at least one contact ($P = 0.012$ Fisher's exact test), and 0.52% of the total mitochondrial surface was engaged in IMJs (Fig. 2*C* and Table S1). This observation suggested that loss of mNEET affects the connectivity of the mitochondrial network by decreasing the formation of IMJs.

We next examined conventional epon-embedded sections by TEM and assessed the frequency of intermitochondrial contacts, defined as regions where two apposed mitochondrial membranes were separated at most by 20 nm (Fig. 3*A*, arrowheads). This technique provides a better resolution than FIB/SEM (lateral resolution, 1 nm) and allows the examination of sections collected from a much larger number of cells. In WT cells, 6.3% of individual mitochondrial sections were apposed to another mitochondrial section (Fig. 3*B* and Table S2), and 0.8% of the mitochondrial surface was engaged into contacts with other mitochondria (Table S2). In sections of mNEET KO cells, the frequency of IMJs was significantly decreased compared with parental cells (only 2.2% of mitochondrial sections exhibited an IMJ, $P = 0.0009$ Fisher's exact test) (Fig. 3*B* and Table S2). The surface of mitochondria involved in IMJs was also strongly decreased (0.4% of the mitochondrial surface engaged in IMJs) (Table S2).

Overall, these observations indicate that genetic ablation of mNEET decreased significantly IMJs, suggesting that mNEET plays a key role in the establishment of IMJs.

www.manaraa.com
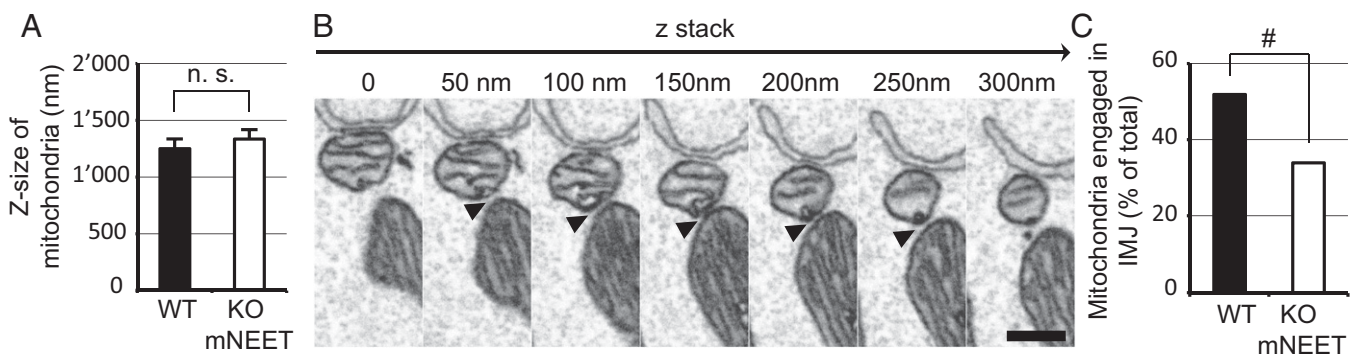
Fig. 2. IMJs are less abundant in *mNEET KO* cells than in WT cells. WT or *mNEET KO* cells were fixed, processed for EM, and analyzed in a Helios Dualbeam SEM to generate complete sets of images scanning the whole-cell volume. Mitochondria from three independent experiments were analyzed for WT and for *mNEET KO* cells. (*A*) The size of mitochondria was evaluated by counting the number of sections through which individual mitochondria extended along the *z* axis (*z*-size) and was not significantly different in WT and *mNEET KO* cells. (*B*) A selection of serial pictures showing an IMJ. Pictures were taken with a 10-nm interval, and one picture every five sections is shown. Arrowheads indicate regions of close contact between two adjacent mitochondria. The distance from each section to the first section shown is indicated. (Scale bar, 50 nm.) (*C*) The percentage of mitochondria engaged in IMJs diminished significantly in *mNEET KO* cells compared with WT cells. #$P = 0.012$ Fisher's exact test; n.s., not significant.

Overexpression of mNEET Increases IMJs. To test further the proposal that mNEET participates in the establishment of IMJs, we assessed the effect of mNEET overexpression in cultured MEF cells. For this, we first transfected transiently mNEET KO cells and assessed the mitochondrial morphology by fluorescence microscopy in cells expressing low levels of mNEET-GFP. In these cells, a tubulated network of mitochondria was restored (Fig. 4 *A* and *B*). This observation confirmed that the fragmentation of mitochondria in mNEET KO cells was caused by the loss of expression of mNEET. Cells expressing high levels of mNEET-GFP were not taken into account in that quantification. In these cells, mitochondria were frequently clustered (Fig. 4*A*), suggesting that overexpression of mNEET-GFP further increased contacts between mitochondria, eventually causing a collapse of the whole mitochondrial network.

To quantify contacts between mitochondria in cells overexpressing mNEET-GFP, WT cells were transfected with mNEET-GFP, sorted by flow cytometry, and fixed 1 d later. Sections were then prepared for observation by conventional TEM. Note that in this experimental set-up, cells expressing moderate-to-high levels of mNEET-GFP were analyzed together. Contacts between mitochondria were much more frequent in cells overexpressing mNEET and mitochondria engaged in contacts with several other mitochondria were commonly observed (Fig. 4*C*). In some instances, zipper-like structures appeared to tether the adjacent mitochondrial membranes at sites of IMJs (Fig. 4*C*, arrowheads). Quantification revealed that more than 40% of individual mitochondrial profiles showed at least one contact (Fig. 4*D* and Table S3). Similarly, the percentage of the mitochondrial surface engaged in IMJs was strongly increased in cells overexpressing mNEET (13%) compared with parental cells (0.8%) (Table S3).

The fact that overexpression of mNEET leads to an increase in IMJs reinforces the suggestion that mNEET participates in tethering of mitochondria and formation of IMJs.

We used the same approach to assess whether the effect of mNEET overexpression was dependent on mitofusins, which are essential for fusion between mitochondria. For this we used *mfn2* KO, as well as *mfn1/2* double-KO MEF cells. Note that unlike the mNEET KO cells described above, these cells are not derived directly from the MEF WT cells used in this study, so that phenotypes of WT, *mfn2 KO*, and *mfn1/2 KO* can at best only be roughly compared. In both cell lines, overexpression of mNEET resulted in a very strong increase in IMJs (Fig. 4 *E* and *F*), indicating that the ability of mNEET to promote formation of IMJs does not require the presence of mitofusins.

Regulation of Mitochondrial Morphology in mNEET KO Cells. Mitochondrial fusion and fission is known to be affected by many physiological parameters. It has been reported previously that in cells exposed to an oxidative stress, the mitochondrial network is rapidly fragmented (14, 15). In contrast, other types of stress, and in particular inhibition of protein synthesis by cycloheximide, result in a marked increase in mitochondrial connectivity (16). In both cases, experimental evidence suggests that changes in the connectivity of the mitochondrial network are a result of changes in the fusion and fission rates of mitochondria that ultimately regulate mitochondrial size. To test the role of mNEET in the response to various stressors, we exposed parental and mNEET KO cells to oxidative stress and to cycloheximide. Exposure to cycloheximide increased the connectivity of the mitochondrial network both in parental and in mNEET KO cells (Fig. 5*A*), suggesting that mNEET does not play a key role in this phenomenon. Conversely, exposure to increasing concentrations of H_2O_2 (from 0.1 to 3 mM) induced a marked decrease in the mitochondrial network connectivity in parental cells (Fig. 5*B*). In mNEET KO cells, the mitochondrial network appeared fragmented already in untreated cells and only a minor decrease in connectivity could be seen in H_2O_2-treated cells (Fig. 5*B*).

Reexpression of mNEET-GFP in mNEET KO cells restored a WT phenotype: the mitochondrial network appeared connected
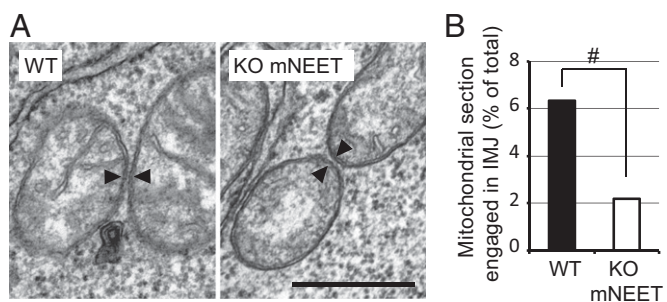
Fig. 3. Conventional EM indicates that the frequency of IMJs is reduced by genetic inactivation of mNEET. WT or *mNEET KO* cells were fixed and sections were visualized in a TEM. (*A*) IMJs were defined as regions of close contact between two mitochondria (<20 nm; arrowheads). (Scale bar, 500 nm.) (*B*) The frequency of IMJs was significantly decreased in *mNEET KO* cells compared with WT cells. #$P = 0.0009$ Fisher's exact test.

Vernay et al.
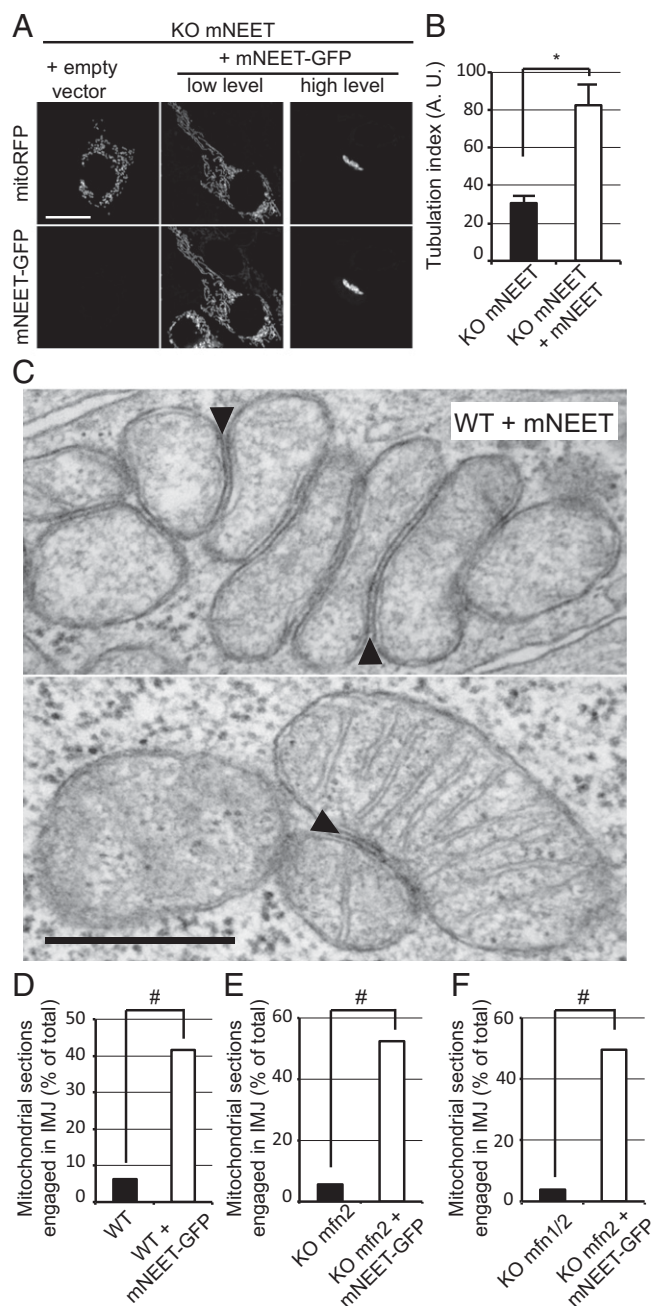
Fig. 4. Overexpression of mNEET increases the connectivity of the mito-chondrial network. (*A*) *mNEET* KO cells were cotransfected with plasmids expressing mitoRFP (*Upper*) and mNEET-GFP (*Lower*). As a control, an empty vector replaced the mNEET-GFP plasmid (*Left*). A mild expression of mNEET-GFP (*Center*) restored the connectivity of the mitochondrial network, whereas a high overexpression (*Right*) resulted in the collapse of the mito-chondrial network. (Scale bar, 10 μm.) (*B*) The connectivity of the mito-chondrial network in cells expressing low levels of mNEET-GFP was determined as described in the legend to Fig. 1. The mean ± SEM of seven independent experiments are presented. *$P < 0.001$ (Student t test). Ex-pression of mNEET-GFP increased the connectivity of the mitochondrial network to a WT level. (*C*) To analyze the effect of mNEET overexpression on IMJs, WT MEF cells were transfected with a plasmid expressing mNEET-GFP. Cells expressing mNEET-GFP were sorted by flow cytometry, and then fixed and processed for EM 1 d later. Arrowheads indicate inter-mitochondrial contacts where electron-dense structures tethering apposed membranes are visible. (Scale bar, 500 nm.) (*D*) The frequency of IMJs was quantified as described in the legend to Fig. 3. IMJs were more abundant in transfected cells than in WT cells. (*E*) The frequency of IMJs was de-termined in *mfn2* KO cells and in *mfn2* KO cells overexpressing mNEET-GFP

and exhibited a decrease in connectivity upon exposure to in-creasing doses of H_2O_2 (Fig. 5*B*).

A mutant form of mNEET (mNEET-4Cys) was characterized previously in which the association of the iron–sulfur cluster with the CDGSH was no longer labile (8, 9). Expression of mNEET-4Cys-GFP in mNEET KO cells resulted in an even higher connectivity of the mitochondrial network (Fig. 5*B*). It also in-creased the resistance of the mitochondrial network to H_2O_2-induced mitochondrial fragmentation to the point where even a treatment with 3 mM H_2O_2 failed to alter significantly the mi-tochondrial network (Fig. 5*B*). These observations suggest that mNEET can participate in the response of the mitochondrial network to oxidizing conditions.

ER–Mitochondria Contact Sites in mNEET KO Cells. In addition to forming IMJs and participating in the connectivity of the mito-chondrial network, mNEET could in principle tether mitochondria to the ER, in particular because the ER contains miner1, a protein highly homologous to mNEET (7). To test this hypothesis, we vi-sualized ER–mitochondria contacts by conventional EM (Fig. 6*A*) and quantified their frequency in WT and in mNEET KO cells, as previously described (17). The perimeter of mitochondrial sections was measured, as well as the zones engaged into close contact with the ER (Table S4). The frequency of ER–mitochondria contacts was not diminished, and actually slightly elevated in mNEET KO cells compared with WT cells (Fig. 6*B* and Table S4). In addition, overexpression of mNEET-GFP did not increase ER–mitochondria contacts (Fig. 6*B* and Table S4). These results indicate that mNEET does not play a critical role in the establishment of ER–mitochon-dria contact sites.

Mitochondrial Respiration in mNEET KO Cells. Finally, we compared mitochondrial respiration in WT and mNEET KO cells. In agreement with previous reports (7), basal and maximal mito-chondrial respiration were reduced by 30% when mNEET was lost (Fig. S3). This defect could reflect a decline in the activity of in-dividual mitochondria, or a decrease in the total amount of cel-lular mitochondria. To distinguish between these two possibilities, we measured on thin sections the percentage of the cell volume occupied by mitochondria. In WT cells, mitochondria occupied 6.45 ± 0.34% of the cytosolic volume, whereas in mNEET KO cells this figure was decreased by 27% (4.74 ± 0.26%; $n = 7$ in-dependent experiments; $P < 0.01$, Mann–Whitney U test) (Table S5). This observation suggests that loss of mitoNEET affects the respiratory capacity of the cell primarily by decreasing the total amount of mitochondria.

Discussion

In this study, we observed and quantified intimate contacts be-tween mitochondria, referred to previously as IMJs (13). No molecular mechanisms have been described so far that ensure close apposition of mitochondria. Our observations strongly sug-gest that mNEET is involved in the formation of IMJs, because the frequency of IMJs is decreased in mNEET KO cells and in-creased in mNEET-overexpressing cells. The most simple mech-anism by which mNEET could participate in the formation of IMJs is by establishing a direct link between two mNEET mole-cules on adjacent mitochondria. Indeed, structural studies have established that mNEET forms dimers and that the linker con-necting the dimerizing CDGSH domain with the mitochondrial membrane exhibits considerable flexibility (18). These features may allow mNEET molecules on neighboring mitochondria to form dimers tethering two adjacent membranes. A more complex

as described above. (*F*) Similar experiments were performed using cells where both mfn1 and mfn2 were genetically inactivated. #$P < 0.001$ Fisher's exact test.

Vernay et al.
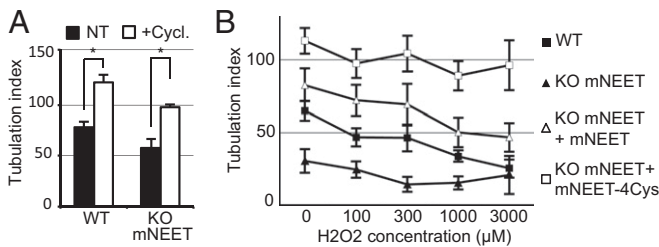
Fig. 5. Regulation of mitochondrial morphology in *mNEET* KO cells. (*A*) WT or *mNEET* KO cells expressing mito-RFP were incubated for 6 h in medium containing 25 μg/mL cycloheximide or not. Cells were then fixed and the connectivity of the mitochondrial network was determined as described in the legend to Fig. 1. The mean ± SEM of three (WT) and eight (*mNEET* KO) independent experiments is indicated. Mitochondrial fusion was stimulated by cycloheximide in both WT and *mNEET* KO cells. NT, not treated. (*B*) WT and *mNEET* KO cells expressing mito-RFP were exposed to various concentrations of H_2O_2 for 1 h. They were then fixed and examined, and degree of connectivity of the mitochondrial network determined. The mean ± SEM of seven (WT) and four (*mNEET* KO) independent experiments is indicated. Mitochondrial connectivity was also determined in *mNEET* KO cells expressing mNEET-GFP, or mNEET-4Cys-GFP.

role of mNEET in formation of IMJs cannot, however, formally be ruled out at this stage. Three lines of evidence suggest that the mechanisms ensuring mNEET-dependent formation of IMJs and fusion/fission of mitochondria are largely distinct. First, the size of mitochondria is unaffected in mNEET KO cells compared with WT cells. Second, mNEET overexpression increases IMJs even in cells devoid of mitofusin 1 and 2. Third, the regulation of fusion/fission by cycloheximide still operates in mNEET KO cells.

To the best of our knowledge, the intermitochondrial contacts observed in this study are identical to or similar to IMJs described recently (13). As previously reported, we observed a close apposition of mitochondrial membranes and in some instances an increase in electron density at the level of intermitochondrial contacts. We also noted that, as previously seen, IMJs are more prominent in some cell types than in others. For example, in HeLa cells, 2.3% of the mitochondrial surface was engaged in IMJs (773 mitochondrial sections analyzed), against 0.8% in MEF cells.

From a methodological point of view, this study exemplifies the power of ultrastructural analysis to assess variations in the morphology of the mitochondrial network. First, EM provides the resolution necessary to delimitate mitochondria, and to visualize IMJs and ER–mitochondria contact sites. Second, ultrastructural analysis is amenable to reliable quantification. Third, recent technical progress in ultrastructural analysis now allows the whole cellular mitochondrial network to be visualized in 3D reconstructions. Quantitative ultrastructural analysis may in some situations be an indispensable tool to understand situations where the mitochondrial network is affected.

Our results provide new indications concerning the cellular function of mNEET and of IMJs. We demonstrate that mNEET plays a role in the formation of the mitochondrial network by mediating the formation of IMJs. Loss of mNEET and the accompanying decrease in IMJs result in a decreased cellular respiration, caused primarily by a decrease in the amount of cellular mitochondria. This result is reminiscent of previous studies reporting that mitochondrial fragmentation (e.g., in mitofusin KO cells) increases autophagy of mitochondria, presumably by altering the mitochondrial membrane potential (19). Our observations suggest that participating in the mitochondrial network, by engaging into mNEET-dependent intermitochondrial contacts, protects individual mitochondrion from degradation by mitophagy. On the other hand, our results did not detect any essential function of mNEET in the function of mitochondria, because mitochondrial respiration, once

corrected for the lower number of mitochondria, was identical in WT and in mNEET KO cells. In addition, our results suggest that the decrease of mitochondrial connectivity in cells exposed to oxidizing conditions is mediated at least in part by mNEET. Indeed, expression of a mutant form of mNEET with a stable FeS cluster rendered the mitochondrial network resistant to oxidative conditions. Previous reports have indicated that mNEET is overexpressed in tumor cells (10) and depleted in cells from cystic fibrosis patients (20). Our results predict that in these pathological conditions, changes in the levels of cellular mNEET could alter the connectivity and the metabolic function of the mitochondrial network. In particular, cancer cells are commonly exposed to oxidative stress (21), and we speculate that overexpression of mNEET may prevent their mitochondrial network from fragmenting.

Finally, small molecules targeting mNEET or miner1 have been characterized (22, 23) and may be used to treat cancer, diabetes, or other pathological conditions. In this perspective, it is essential to understand fully the cellular functions of mNEET, miner1, and miner2 to determine the effects of such compounds on cellular physiology. Our results suggest that compounds targeting mNEET may affect the formation of IMJs as well as the stability of mitochondria. The functional consequences of such alterations at the cellular and at the organism level remain to be established.

Materials and Methods

Cell Culture and Reagents. MEF cells were grown in DMEM supplemented with 10% FBS, penicillin-streptomycin, and nonessential amino acids.

To visualize the mitochondrial network, cells were grown on 20-mm glass coverslips and transfected with mitoRFP 2 d before the experiment, using polyethylenimine, as described previously (24). Cells were then directly fixed in 4% paraformaldehyde for 30 min, permeabilized with 0.2% saponin, washed in PBS, and mounted in Möwiol. Fluorescence was imaged by confocal microscopy (LSM700, Zeiss). When challenged with an oxidative stress, cells were treated for 1 h with hydrogen peroxide before fixation. Hyperfusion of mitochondria was induced by incubating the cells in the presence of 25 μg/mL cycloheximide for 6 h before fixation.

The plasmid allowing overexpression of mNEET-GFP is based on a pEGFP-N1 backbone (7) and was a kind gift of S. E. Wiley, University of California, San Diego.
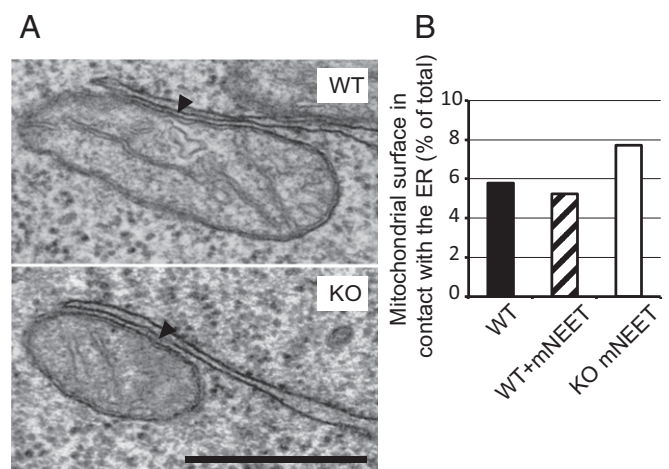
Fig. 6. Establishment of ER–mitochondrial contact sites is independent on mNEET. (*A*) WT, *mNEET* KO, or mNEET-overexpressing cells were fixed and processed for conventional EM. Sites of juxtaposition of ER and mitochondrial membranes were visualized (arrowheads), and quantified. (Scale bar, 500 nm.) (*B*) Approximately 6% of mitochondrial membrane was engaged into contacts with the ER in WT cells. This figure did not change significantly in cells overpressing mNEET, and increased slightly in *mNEET* KO cells.

Vernay et al.

Generation of mNEET KO Cell Lines. We generated *mNEET*-knockout cell lines using the CRISPR/Cas9 method, as described previously (25). Briefly, a plasmid purchased from DNA2.0 was used, the guide RNA targeting the first exon of *mNEET* (AGCTCCAACTCCGCTGT*GCGAG; the * represents the cutting site of the Cas9 nuclease). Eight individual clones were screened for mutations by PCR. We amplified 500-bp upstream and downsteam the cutting site on the genomic DNA (purified using the QIAamp DNA Blood MiniKit; Qiagen) using the following primers: primer 1, 5′-GTGTAACTTAT-TACCAAAAGT-3′, and primer 2, 5′-CAGTCAGTCACGCATATC-3′. Fragments obtained were then purified and sequenced. Three individual clones were obtained with indels inducing a frameshift in both alleles. These three clones were used in parallel with very similar results.

Fluorescence Microscopy. A recombinant antibody against mNEET (MRB251) was generated as described previously (26) by the Geneva Antibody Facility (https://www.unige.ch/medecine/anticorps/recombinant-antibodies/). The mitochondrial network was revealed either by mitoRFP or by mNEET-GFP, as indicated. Importantly, all quantifications were performed on blinded samples to avoid experimental biases. As shown on Fig. S2A, for each sample we examined 150–200 individual cells, and scored the aspect of the mitochondrial network (4: totally fragmented; 3: partially fragmented; 2: tubular; 1: hyperconnected). To summarize this result into a single number, we calculated the tubulation index: $2 \times$ (percentage of cells with an hyperconnected network) + (percentage of cells with a tubular network) + $0.5 \times$ (percentage of cells with a partially fragmented network).

Electron Microscopy. To obtain Epon-embedded sections for conventional EM, cells we grown in 35-mm plastic dishes, fixed with 0.1 M sodium phosphate, pH 7.4 containing 2% glutaraldehyde, postfixed with osmium tetroxide, stained with uranyl acetate, dehydrated in ethanol, and embedded in Epon resin. After sectioning, the samples were observed in a Morgagni EM. The iTEM software was used for quantification.

To generate high-resolution 3D reconstructions, we analyzed samples using a Helios DualBeam NanoLab 660 SEM. Images were further analyzed using the AMIRA software. To evaluate the size of mitochondria, we counted for each mitochondrion the number of sections through which it extended to determine its size along the *z* axis (*z*-size). We also determined the number of sections that each IMJ traversed. The ratio of these two figures indicated the percentage of the mitochondrial surface engaged into contacts.

Mitochondrial Respiration. The oxygen consumption rate was measured using an XF96 extracellular analyzer (Seahorse Bioscience) according to the manufacturer's protocol. Briefly, 10,000 cells were seeded in 96-well plates for 24 h in culture medium. Cells were then incubated in Krebs-Ringer bicarbonate Hepes buffer (KRBH, 135 mM NaCl, 3.6 mM KCl, 10 mM Hepes, pH 7.4, 2 mM NaHCO₃, 0.5 mM NaH₂PO₄, 0.5 mM MgCl₂, 1.5 mM CaCl₂ supplemented with 10 mM glucose) for 45 min at 37 °C in a non–CO₂ incubator. Cells were then transferred into a Seahorse analyzer at 37 °C and were sequentially treated with 1 μM oligomycin, 300 nM carbonyl cyanide-*p*-trifluoromethoxyophenylhydrazone (FCCP), and a 0.5 μM mixture of rotenone and antimycin A. Oxygen consumption rate was automatically measured after addition of each compound, as the average of two readings from nine wells. At the end of each experiment, the amount of protein in each well was quantified, and the oxygen consumption values were corrected to avoid differences caused by variations in the number of cells.

1. Montgomery MK, Turner N (2015) Mitochondrial dysfunction and insulin resistance: An update. *Endocr Connect* 4:R1–R15.
2. Giampazolias E, Tait SW (2016) Mitochondria and the hallmarks of cancer. *FEBS J* 283:803–814.
3. Archer SL (2013) Mitochondrial dynamics–Mitochondrial fission and fusion in human diseases. *N Engl J Med* 369:2236–2251.
4. Hoppins S, Lackner L, Nunnari J (2007) The machines that divide and fuse mitochondria. *Annu Rev Biochem* 76:751–780.
5. Colca JR, et al. (2004) Identification of a novel mitochondrial protein ("mitoNEET") cross-linked specifically by a thiazolidinedione photoprobe. *Am J Physiol Endocrinol Metab* 286:E252–E260.
6. Colca JR, et al. (2013) Identification of a mitochondrial target of thiazolidinedione insulin sensitizers (mTOT)—Relationship to newly identified mitochondrial pyruvate carrier proteins. *PLoS One* 8:e61551.
7. Wiley SE, Murphy AN, Ross SA, van der Geer P, Dixon JE (2007) MitoNEET is an iron-containing outer mitochondrial membrane protein that regulates oxidative capacity. *Proc Natl Acad Sci USA* 104:5318–5323.
8. Wiley SE, et al. (2007) The outer mitochondrial membrane protein mitoNEET contains a novel redox-active 2Fe-2S cluster. *J Biol Chem* 282:23745–23749.
9. Zuris JA, et al. (2011) Facile transfer of [2Fe-2S] clusters from the diabetes drug target mitoNEET to an apo-acceptor protein. *Proc Natl Acad Sci USA* 108:13047–13052.
10. Sohn YS, et al. (2013) NAF-1 and mitoNEET are central to human breast cancer proliferation by maintaining mitochondrial homeostasis and promoting tumor growth. *Proc Natl Acad Sci USA* 110:14676–14681.
11. Kusminski CM, et al. (2012) MitoNEET-driven alterations in adipocyte mitochondrial activity reveal a crucial adaptive process that preserves insulin sensitivity in obesity. *Nat Med* 18:1539–1549.
12. Kusminski CM, et al. (2016) MitoNEET-Parkin effects in pancreatic α- and β-cells, cellular survival, and intrainsular cross talk. *Diabetes* 65:1534–1555.
13. Picard M, et al. (2015) Trans-mitochondrial coordination of cristae at regulated membrane junctions. *Nat Commun* 6:6259.
14. Jendrach M, Mai S, Pohl S, Vöth M, Bereiter-Hahn J (2008) Short- and long-term alterations of mitochondrial morphology, dynamics and mtDNA after transient oxidative stress. *Mitochondrion* 8:293–304.
15. Iqbal S, Hood DA (2014) Oxidative stress-induced mitochondrial fragmentation and movement in skeletal muscle myoblasts. *Am J Physiol Cell Physiol* 306:C1176–C1183.
16. Tondera D, et al. (2009) SLP-2 is required for stress-induced mitochondrial hyperfusion. *EMBO J* 28:1589–1600.
17. Cosson P, Marchetti A, Ravazzola M, Orci L (2012) Mitofusin-2 independent juxtaposition of endoplasmic reticulum and mitochondria: An ultrastructural study. *PLoS One* 7:e46293.
18. Conlan AR, et al. (2009) The novel 2Fe-2S outer mitochondrial protein mitoNEET displays conformational flexibility in its N-terminal cytoplasmic tethering domain. *Acta Crystallogr Sect F Struct Biol Cryst Commun* 65:654–659.
19. Twig G, Shirihai OS (2011) The interplay between mitochondrial dynamics and mitophagy. *Antioxid Redox Signal* 14:1939–1951.
20. Taminelli GL, et al. (2008) CISD1 codifies a mitochondrial protein upregulated by the CFTR channel. *Biochem Biophys Res Commun* 365:856–862.
21. Panieri E, Santoro MM (2016) ROS homeostasis and metabolism: A dangerous liason in cancer cells. *Cell Death Dis* 7:e2253.
22. Bai F, et al. (2015) The Fe-S cluster-containing NEET proteins mitoNEET and NAF-1 as chemotherapeutic targets in breast cancer. *Proc Natl Acad Sci USA* 112:3698–3703.
23. Geldenhuys WJ, Leeper TC, Carroll RT (2014) mitoNEET as a novel drug target for mitochondrial dysfunction. *Drug Discov Today* 19:1601–1606.
24. Longo PA, Kavran JM, Kim MS, Leahy DJ (2013) Transient mammalian cell transfection with polyethylenimine (PEI). *Methods Enzymol* 529:227–240.
25. Perrin J, et al. (2015) TM9 family proteins control surface targeting of glycine-rich transmembrane domains. *J Cell Sci* 128:2269–2277.
26. Blanc C, Zufferey M, Cosson P (2014) Use of in vivo biotinylated GST fusion proteins to select recombinant antibodies. *ALTEX* 31:37–42.

Vernay et al.

www.manaraa.com